Original Article

Multimodal Imaging in Retinitis Pigmentosa: Correlations among Microvascular Changes, Macular Function and Retinal Structure

Yousra Falfoul[1,2], Issam Elleuch[1,2], Khaled El Matri[1,2], Hela Ghali[3], Asma Hassairi[1,2], Ahmed Chebil[1,2], Nibrass Chaker[1,2], Leila El Matri[1,2]

[1]B Department, Oculogenetic Laboratory LR14SP01, Tunis El Manar University, Tunis, Tunisia, [2]Department of Ophthalmology, Hédi Raies Institute of Ophthalmology, Faculty of Medicine of Tunis, Tunis, Tunisia, [3]Department of Family and Community Medicine, Faculty of Medicine Ibn El Jazzar Sousse, Sousse, Tunisia

Abstract

Purpose: To analyze microvascular changes in patients with retinitis pigmentosa (RP) with relatively preserved visual acuity (VA), using swept source optical coherence tomography (SS-OCT) angiography to correlate results to macular function and structure.

Methods: This was a case–control study conducted over 70 eyes of 35 RP patients with relatively preserved VA. All patients underwent a complete ophthalmic examination, including SS-OCT, OCT angiography (OCT-A), fundus autofluorescence (FAF), and multifocal electroretinogram (mfERG). Thirty-four eyes of 34 healthy controls of age-, sex-, and axial length-matched (control group), were also analyzed. The main outcome measures were foveal and parafoveal vascular densities (FVDs and PFVDs) in the superficial capillary plexus (SCP) and deep capillary plexus (DCP), foveal avascular zone (FAZ) and its enlargement coefficient and their correlation with macular function (by means of VA and mfERG), and structure (by means of FAF and SS-OCT).

Results: In the RP group, PFVD was 25.99 ± 5.2% in the SCP and 34.47 ± 2.37% in the DCP and were significantly lower as compared to control group ($P < 0.0001$; $P = 0.0026$, respectively). Enlargement coefficient of FAZ was 1.78 ± 0.79. We found a statistically significant correlation between VA and PFVD in the DCP ($P < 0.0001$), FAZ disruption in the SCP ($P = 0.006$) and enlargement coefficient of FAZ ($P = 0.01$). The parafoveal DCP density was significantly correlated with P1 amplitude ($P = 0.005$) in rings 2, 3, 4, and 5 of the mfERG. We found a statistically significant correlation between parafoveal density in the DCP, thickness of ganglion cell complex (GCC) ($P = 0.001$), and the width of ellipsoid band ($P = 0.041$). Parafoveal SCP density was also correlated to GCC ($P = 0.033$).

Conclusions: We showed that vascular alteration in RP begins at the level of the DCP, which affects the outer retina and leads to a narrowing of the ellipsoid. The alteration of the SCP would occur later in the evolution of the disease. Vascular changes occur early during RP and were highly correlated to retinal function and structure. OCT-A seems to be a good tool to quantify vascular network loss and could play a central role in staging, prognosis, and monitoring disease progression.

Keywords: Multimodal functional and structural imaging, Optical coherence tomography angiography, Retinitis pigmentosa, Vascular density

Address for correspondence: Yousra Falfoul, Department of Ophthalmology, Hédi Raies Institute of Ophthalmology, Faculty of Medicine of Tunis, Tunis, Tunisia.
E-mail: yosra.falfoul@yahoo.fr
Submitted: 19-Aug-2019; **Revised:** 14-Nov-2019; **Accepted:** 08-Dec-2019; **Published:** 30-Apr-2020

Introduction

Retinitis pigmentosa (RP) is a group of inherited retinal diseases, in which the primum movens is an alteration of retinal pigment epithelium (RPE)-photoreceptors complex.[1-3] Loss of rods associated with the degeneration of RPE cells leads to the accumulation of pigmented deposits at the retinal periphery and subsequently to a progressive loss of peripheral visual field and nyctalopia; subsequent cone degeneration leads

Access this article online

Quick Response Code:

Website: www.jcurrophthalmol.org

DOI: 10.4103/JOCO.JOCO_99_20

How to cite this article: Falfoul Y, Elleuch I, El Matri K, Ghali H, Hassairi A, Chebil A, *et al*. Multimodal imaging in retinitis pigmentosa: Correlations among microvascular changes, macular function and retinal structure. J Curr Ophthalmol 2020;32:170-7.

to a decrease in macular function. The main changes occur at the level of the outer retina[3]; however, in recent tomographic studies, using optical coherence tomography (OCT), there is an increasing evidence that the inner retina, mainly the retinal ganglion cell, may also be involved with the progression of RP. Furthermore, in many histopathological studies, vascular changes in the retinal and choroidal vessels have been implicated in RP pathogenesis and progression,[4,5] but it is not clear yet whether the vascular component is primitive or secondary to photoreceptor degeneration.

OCT angiography (OCT-A) is a non-invasive method that has been recently developed to study both retinal and choroidal microvasculature. Qualitative and quantitative evaluation of the vascular bed in both the superficial and deep capillary plexuses (SCPs and DCPs) may help finding a possible correlation between vascular perfusion and retinal structure and function.

Several reports[3-5] studied the role of microvascular alterations in RP, but it is still not clear whether vascular changes start before or after structural changes. The aim of this study was to assess the relationships between macular structure, function, and vascular changes in RP patients at an early- and mid-stage of the disease to better understand the role of microvascular changes in RP. We evaluated both macular function (by means of best corrected visual acuity [BCVA] and multifocal electroretinogram [mf-ERG]), and structure (by means of fundus autofluorescence [FAF] and swept source OCT [SS-OCT]) and we investigated the retinal microvascular changes by means of OCT-A.

Methods

This was a case–control study. Thirty-five patients (70 eyes) diagnosed with either early- or mid-stage rod cone RP and 35 controls were assessed at Hédi Rais Institute of Ophthalmology (HRIO), Tunis, Tunisia. The HRIO Ethics Committee approved the study and all patients gave consent to the use of their data. The study complied with all tenets of the Declaration of Helsinki.

The diagnosis of RP was made based on clinical and multimodal imaging examination completed with visual field or full-field ERG if necessary.

Only patients with a BCVA of at least one logMAR were enrolled in the study to ensure good fixation, and to minimize motion artifacts during examinations.

Exclusion criteria were refractive error <−6 D or > +6 D; evidence of an advanced form of RP (either undetectable ERG or extended macular atrophy), cone rod dystrophy or stationary disorder; any retinal disease affecting the patient other than RP; a history of ocular hypertension, glaucoma, or any condition increasing the risk of secondary glaucoma; patients under medication that may alter the retinal vasculature; segmentation errors caused by an important macular edema or by a fibrous proliferation with an evidence of macular traction and media opacities that may obstruct the visualization of the retinal vascular network.

All patients underwent a complete ocular examination, including visual acuity (VA), Intraocular pressure (IOP) measurement, fundus examination, FAF, SS-OCT, OCT-A, A and B ocular echography, and mfERG. An age- and sex-matched control group of 34 eyes of 34 healthy controls was also included in the current analysis. All controls also underwent an ophthalmologic evaluation, including BCVA, IOP, fundus examination, OCT, and OCT-A.

All scans were performed by a trained ophthalmologist using a Topcon Swept source DRI OCT-A Triton® (Topcon, Tokyo, Japan). Before imaging, each of the subjects' pupils were dilated. We used an internal fixation light to center the scanning area. We used the "OCT-A" function, while enabling the automatic eye tracking function, to obtain 3 mm × 3 mm OCT raster scans of the fovea. We used the automated segmentation tool to get four images of the SCP, DCP, outer retina, and the choriocapillaris (CC). Boundaries of the SCP and DCP slabs for the OCT-A measurements were automatically segmented according to the manufacturer's default settings. The SCP slab was segmented from an inner boundary at 2.6 mm beneath the inner limiting membrane and an outer boundary at 15.6 mm beneath the inner plexiform layer (IPL). The DCP slab was obtained with a slab between the inner and outer boundaries, respectively, at 15.6 and 70.2 mm beneath the IPL.

In cases were the image quality was deemed inadequate due to motion blur, or the acquisition not centered on the fovea due to poor fixation, we performed another OCT-A acquisition. If the image quality remained inadequate, the corresponding patients were excluded from the study. Two investigators checked the segmentation quality before testing the vessel (Y. F. and I. E.) and performed manual measurements independently at different timepoints and in different orders. In instances of disagreement, there was open adjudication between the two readers until a consensus was established. After selecting the images with the best resolution, the foveal avascular zone (FAZ) area was manually outlined using the freehand selection tool in both SCP and DCP with the IMAGEnet® digital imaging system (Topcon Medical Systems, Oakland, NJ, USA). Its dimension was expressed in squared millimeters. Quantitative analysis was performed on the OCT-A enface images for each eye using the National Institutes of Health ImageJ 1.50 software (National Institutes of Health, Bethesda, Maryland, USA).

Both SCP and DCP OCT-A images were retrieved from the system as Joint Photographic Experts Group file to ImageJ. The 3 mm × 3 mm image were set to a scale of 320 × 320 pixels and then binarized to an image containing only white and black pixels. The binarized OCT-A images were skeletonized, showing the blood vessels as a 1-pixel-wide line, and ImageJ was used to count the number of black pixels and total pixels. Foveal vascular density (FVD) in both SCP and DCP was obtained by analyzing pixels inside a 1 mm diameter circle centered on the foveal center. The vascular density (VD) inside

a 3 mm circle centered on the fovea was also measured; the parafoveal VD (PFVD) is then measured by deducting the foveal density from the total VD inside the 3 mm circle using this mathematical formula:

([(A × C)/100-(B × D)/100]/[A-B]) × 100

- A: Area of the 3 mm drown circle centered on the fovea in mm 3
- B: Area of the 1 mm drown circle centered on the fovea in mm 3
- C: VD expressed in % inside the 3 mm circle
- D: VD expressed in % inside the 1 mm circle.

The FVD and PFVD were defined as the VD in the foveal region with a diameter of 1 mm and the parafoveal region with a diameter from 1 mm to 3 mm [Figure 1].

In the qualitative analysis, FAZ integrity was assessed, FAZ disruption was defined by the presence of gaps or interruption of the capillary ring leading to a loss of blood vessels integrity which form an irregular circle.

Cross-sectional structural OCT scans were acquired afterward using the same instrument (DRI OCT Triton, Topcon, Tokyo, Japan) following a protocol that included the DRI OCT 3D macula set of 7 mm × 7 mm and the (H) line function. We studied them and looked for the inner/outer retinal atrophy, epiretinal membrane, hyperreflective foci of the outer retina, and the presence of hyporeflective intraretinal spaces.

Outer retinal atrophy was defined as the loss of the integrity of the external limiting membrane (ELM), ellipsoid zone (EZ), and interdigitation zone bands and inner retinal atrophy by decreased retinal nerve fiber layer, ganglion cell layer (GCL), and IPL thicknesses.

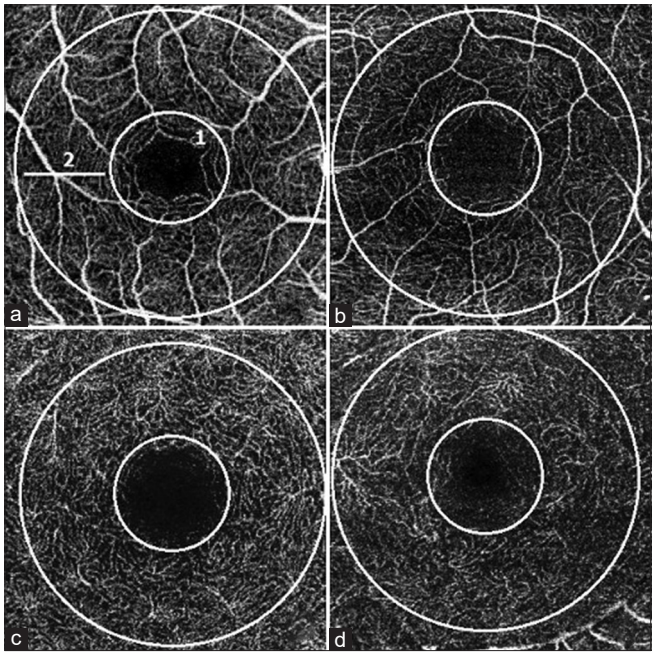

Figure 1: Examples of retinal optical coherence tomography angiography angiograms of the superficial plexus in control (a) and retinitis pigmentosa (RP) patients (b) and of the deep plexus in normal (c) and RP (d). The foveal flow density (1: Diameter of 1 mm [small white circle]), parafoveal flow density (2: Diameter from 1 to 3 mm) were analyzed

For the appreciation of the external ELM and ellipsoid band, grey scale images were used for a more precise identification and measurements. The structure of the ellipsoid band in three areas (subfoveal, peri foveal, and parafoveal), was graded from 1 to 3: Grade 1, ellipsoid not visible; Grade 2, abnormal or incomplete ellipsoid; and Grade 3, normal and complete ellipsoid. The same grading system was used to appreciate the ELM. When the ellipsoid was visible and its width did not exceed the scanned images, its width was measured between the borders where the ellipsoid band met the upper surface of the RPE using the built-in caliper. If the ellipsoid band width exceeded the scanned images, its length was not measured, and its dimension was set to "complete."

The average of the ellipsoid width of the horizontal images was used for the statistical analyses. Two of the authors (Y. F. and I. E.) who were masked to the VA confirmed the grade of the ellipsoid.

Center and average macular thicknesses were automatically rendered by the DRI-OCT software. For ganglion cell complex (GCC) thickness evaluation, we used the GCC 6 mm × 6 mm thickness map, which contains an elliptical annulus, centered on the fovea.

For choroidal thickness (CT) evaluation, we manually measured the distance between the RPE and the inner scleral wall, in 21 different locations in each eye, starting subfoveally, and extending nasally, superiorly, inferiorly, and temporally by incrementing 500 μ until reaching 2500 μ away from the subfovea in each direction. The CT corresponded to the average of 21 measurements. CT was measured in all patients between 10 a.m and 1 p.m to discard nycthemeral fluctuation.

FAF images were obtained using a confocal scanning laser ophthalmoscope (Heidelberg Spectralis; Heidelberg-Engineering, Heidelberg, Germany). We divided the subjects into three subgroups based on the macular FAF results, as previously reported: Type 1: No abnormal ring-shaped hyperautofluorescence (HAF) or foveal HAF; Type 2: A complete or incomplete ring-shaped HAF; type 3: Abnormal foveal HAF.

The vertical, horizontal, and area dimensions for each hyperautofluorescent ring were measured along the inner boundaries of the ring. In cases involving a hyperautofluorescent arc rather than a complete ring, or a nasal edge of the ring that passes through or fell outside the optic disc, only one axis was measured and the other dimensions were set to "missing."

Two of the authors (Y.F. and I.E.) were blinded to the patients' clinical characteristics performed the classification and the measurements. In addition, we examined patchy areas of hypoautofluorescence in mid-periphery and areas of hypoautofluorescence around the optic disc, previously

reported in RP.[6] Eyes were categorized according to the presence and the absence of these lesions.

Multifocal ERG (Métrovision, France) was recorded for each patient according to the International Society for Clinical Electrophysiology of Vision standards. The stimulus was an array of 61 hexagons that were scaled according to eccentricity and changed with a frequency of 120 Hz. The luminance of the white hexagons was 400 cd/m^2, the luminance of the black hexagons was inferior to 4 cd/m^2, and the surround luminance was 30 cd/m^2. The amplitudes of N1 (first negative component) and P1 (first positive component) of the first-order kernel were calculated for five regional ring groups (R1, R2, R3, R4, and R5).

OCT-A, SS-OCT, autofluorescence (AF), and mfERG measurements were performed at the same time as the visual testing.

All statistical analyses were performed using the Statistical Package for the Social Sciences (version 21.0; SPSS, Inc., Chicago, IL, USA). BCVA data were converted to the logMAR for the statistical analyses. All qualitative variables were summarized as frequency and percentage.

OCT-A vessel densities and OCT thicknesses were compared to the control group, we correlated other imaging with OCT-A and OCT only in RP eyes.

Statistical significance in the differences between two qualitative variables was assessed using Fischer's exact test or Chi-square test, depending on the examined sample size.

To detect departures from normality distribution, Shapiro–Wilk's test was performed overall quantitative variables. Absolute and relative frequencies were measured for qualitative variables.

All quantitative variables were summarized as mean, standard deviation, and minimum and maximum values where they had a normal distribution, and were compared to qualitative variables using Student's *t*-test when two groups are to be compared or analysis of variance when more than two groups are to be compared. Otherwise, they were summarized as median, 25th, and 75th percentile and were compared to quantitative variables using the Mann–Whitney's correlation test.

The linear correlation among quantitative variables in RP patients was studied using bivariate correlation test. We used Pearson's correlation coefficient® for cohorts < 30 and Spearman's correlation coefficient for cohorts > 30. A $P < 0.05$ was considered statistically significant.

Results

The mean age of RP patients was 31.91 years ± 13.18 with a range of 9–60 years and 71.4% of patients were younger than 40 years. In controls, mean age was 35 years old ± 15 with a range of 11–66 years old ($P = 0.069$). Sex ratio was 1.18 in RP patients and 0.90 in controls ($P = 0.058$). Inheritance was autosomal recessive in 26 patients, dominant in 2 patients and sporadic in 7 patients.

Mean age at disease onset was 14 years with a range of 1–50 years and mean duration of the disease was 13 years (6.75–24). Mean BCVA of RP patients was 0.301 (0.154–0.397) (logMAR).

Foveal SCP VD was 8.65 ± 4.42% in the RP group and 10.89 ± 3.63% in the control group ($P = 0.0417$). Moreover, the parafoveal SCP VD was reduced in RP patients (25.99 ± 5.2% and 29.74 ± 3%; $P = 0.0026$). FAZ disruption was present in 17.7% of the cases.

Cystoid spaces were present in 1.5% of cases in the SCP; all had no decorrelation signal on their wall.

FAZ area in the DCP was 575.96 µm² ± 162.94 and 362 µm² ± 107 in the control group ($P < 0.0001$).

Foveal DCP VD was 2.82 ± 2.51% in the RP group and 8.02 ± 4.96% in the control group ($P < 0.0001$). Moreover, the parafoveal DCP VD was reduced in RP patients (25.04 ± 5.53% and 34.47 ± 2.37%; $P < 0.0001$). FAZ disruption was present in 11.8% of cases. Cystoid spaces were observed in the DCP in 30.8% of cases, 9.6% had a decorrelation signal on their wall and 21.2% had no signal.

Enlargement coefficient of FAZ was 1.78 ± 0.79.

Mean foveal thickness and GCC were significantly lower in RP group, all values are summarized in Table 1.

A similar architecture of the macula was found in all our patients, the structurally intact foveal center extends in a centrifugal manner toward: first a region characterized by thinning of the photoreceptor outer segments, second a region where both outer segments and outer nuclear layer become thin. Third a region where there is total loss of both outer

Table 1: Structural optical coherence tomography and optical coherence tomography angiography measurements in retinitis pigmentosa patients and controls

	RP group	Controls	Significance level (*P*)
FAZ area SCP (µm²)	369.69±142	312±119	0.10*
Foveal SCP VD (%)	8.65±4.42	10.89±3.63	**0.0417***
Parafoveal SCP VD (%)	25.99±5.2	29.74±3	**0.0026***
FAZ area DCP (µm²)	575.96±162.94	362±107	**<0.0001***
Foveal DCP VD (%)	2.82±2.51	8.02±4.96	**<0.0001***
Parafoveal DCP VD (%)	25.04±5.53	34.47±2.37	**<0.0001***
Mean foveal thickness (µm)	236.3±38.2	274±12.2	**0.0002***
GCC (µm)	72.86±21	108±5.3	**<0.0001***
Choroidal thickness (µm)	240.5±90.8	241±65.4	0.766*
Center foveal thickness (µm)	198 (162-336)	187.8±17.7	0.09[ł]

Data are expressed as mean and standard deviation if normal distribution, or in median, 25th, and 75th percentile. *Student's *t*-test, [ł]Mann-Whitney's correlation test. Bold indicates significant values. RP: Retinitis pigmentosa, FAZ: Foveal avascular zone, SCP: Superficial capillary plexus, VD: Vascular density, DCP: Deep capillary plexus, GCC: Ganglion cell complex

segments and ellipsoid. Finally, to a fourth region where a very thin outer nuclear layer is directly in contact with the pigment epithelium. The structural analysis in SS-OCT revealed central macular edema (CME) in 54.3 of cases, outer retinal atrophy in 20%, inner retinal atrophy in 34.3%, and hyperreflective foci of the outer retina in 15.7% of eyes. Foveal ELM was absent in 2.9%, partially present in 37.1%, and complete in 59.4% of the cases.

The width of the EZ, whenever it was complete, was 2273.9 μm ± 1177.8. We found that the width of the ELM was always greater than the ellipsoid's width. Mean foveal thickness was 236.3 μm ± 38.2 in RP patients and 274 μm ± 12.2 in healthy controls ($P = 0.0002$). In patients without CME, center foveal thickness was 166 μm ± 48 and 187.8 μm ± 17.7 in controls ($P = 0.09$). Average GCC thickness was significantly lower in RP patients (72.86 ± 21 and 108 ± 5.3; $P < 0.0001$). CT was 240.5 ± 90.8 in RP patients and 241 ± 65.4 in controls.

Table 2 summarizes P1 and N1 values in RP group in different areas of mfERG.

FAF was normal in 10.8% of the cases, abnormal foveal HAF in 12.3% and an HAF ring was observed in 76.9% of the cases. Patchy hypofluorescence of the mid-periphery was observed in 40% of the cases, a peripapillary hypofluorescence in 53.8% of the cases and retinal vessel attenuation in 60% of the cases.

In patients with HAF ring, the ring was incomplete in 12% of the cases. The HAF ring was located within a circle of 1500 microns' diameter in 22% of the cases, between two circles of 1500 and 3000 μ in diameters in 40% of the cases and beyond a 3000 μ diameter circle in 38% of cases.

In cases of HAF ring, width of the horizontal diameter of the HAF ring was 2583.4 μ ± 1258.4, width of the vertical diameter of the HAF was 2007.5 μm ± 976, and average area of HAF ring was 4.86 mm² ± 4.32.

PFVD in the SCP and DCP were significantly correlated to GCC thickness and PFVD in the DCP was significantly correlated with the EZ width.

Table 3 highlights different correlations studied between VD, GCC thickness, and ellipsoid band width. PFVD in the DCP was significantly correlated with P1R2 ($P = 0.008$); P1R3 ($P = 0.013$); P1R4 ($P = 0.016$); and P1R5 ($P = 0.005$) but not with P1R1 ($P = 0.112$).

We found statistically significant correlation between enlargement coefficient of FAZ, its area in the SCP ($P = 0.004$) and PFVD in the DCP ($P < 0.01$).

BCVA was significantly correlated with the PFVD in the DCP ($P < 0.0005$). Table 4 summarizes different correlations studied between BCVA and different parameters in OCT-A, SS-OCT and FAF. BCVA was significantly correlated with the GCC thickness ($P = 0.012$), and with mean macular thickness in patients with no CME ($P = 0.03$). BCVA was not significantly correlated with the width of the ellipsoid, otherwise, BCVA was

Table 2: N1 (first negative component) and P1 (first positive component) measurements in multifocal electroretinogram in retinitis pigmentosa patients

	Mean	Maximum	Minimum	SD
N1 area 2	−179.15	202	−702	186.6
N1 area 3	−163.44	42	−688	149.48
N1 area 4	−134.95	72	−588	135.95
N1 area 5	−124.71	32	−519	125.26
P1 area 1	748.16	2489	107	498.32
	Median	**25th percentile**		**75th percentile**
N1 area 1	−354	−453		−203
P1 area 2	293	200		398
P1 area 3	185	124.5		299
P1 area 4	186.5	116.25		302.75
P1 area 5	176.5	89.5		271.25

Data are expressed as mean and SD, median and and 25th and 75th percentile. SD: Standard deviation; N1: First negative component; P1: First positive component

Table 3: Correlations between vessel densities and ganglion cell layer thickness and ellipsoid band width in retinitis pigmentosa patients

	GCC (*P*)	EZ width (*P*)
SCP FVD	0.319	0.292
SCP PFVD	**0.033**	0.103
DCP FVD	0.597	0.440
DCP PFVD	**0.001**	**0.041**

Spearman's correlation coefficient was performed to evaluate the linear correlation among variables. Bold indicates significant values. GCC: Ganglion cell complex, EZ: Ellipsoid zone, SCP: Superficial capillary plexus, FVD: Foveal vascular density, PFVD: Parafoveal vascular density, DCP: Deep capillary plexus

correlated with the presence of EZ retrofoveally ($P = 0.001$), perifoveally ($P = 0.010$), and parafoveally ($P < 0.0001$). Mean BCVA was 0.301 (0.096–0.301) in patients without CME and 0.301 (0.154–0.566) in patients with CME, and the correlation of BCVA with the presence of CME was not statistically significant ($P = 0.082$). Both mean and center foveal thicknesses were not significantly correlated with BCVA ($P = 0.757$; $P = 0.408$, respectively), meanwhile mean foveal thickness in patients not having CME was significantly correlated with BCVA ($P = 0.03$). Both mean and center foveal thicknesses were significantly correlated with the width of ellipsoid ($P < 0.0005$). The duration of disease progression was not correlated with EZ width but was correlated with both CT ($P = 0.002$) and BCVA ($P = 0.001$). Ellipsoid width was correlated with both vertical ($P < 0.0005$) and horizontal ($P < 0.0005$) diameters of the HAF ring.

The presence of hyperreflective foci of the outer retina was not correlated with the width of the EZ, but was significantly correlated with the absence of the EZ ($P = 0.001$), in fact, 71.4% of patients having foci did not have a measurable EZ width compared to 9.7% having an identifiable EZ.

Table 4: Different correlations studied between best corrected visual acuity and different parameters in optical coherence tomography angiography, swept source optical coherence tomography and fundus autofluorescence in retinitis pigmentosa patients

	BCVA		
FVD in the SCP	*P*=0.165	FVD in the DCP	*P*=0.246
PFVD in the SCP	*P*=0.139	FVD in the DCP	***P*<0.0005**
FAZ area in the SCP	*P*=0.498	FAZ area in the DCP	*P*=0.235
FAZ interruption in the SCP	***P*=0.006**	FAZ interruption in the DCP	*P*=0.336
Presence of cystoid spaces in the SCP	*P*=0.083	Presence of cystoid spaces in the DCP	***P*=0.003**
FAZ enlargement ratio	***P*=0.017**		
OR atrophy	***P*=0.006**	GCC thickness	***P*=0.012**
IR atrophy	***P*=0.016**	Presence of CME	*P*=0.082
EZ width	*P*=0.441	CMT	*P*=0.408
EZ present retro foveally	***P*=0.001**	MMT	*P*=0.757
EZ present peri foveally	***P*=0.010**	MMT (no CME group)	***P*=0.03**
EZ present parafoveally	***P*<0.0001**	Choroidal thickness	*P*=0.893
Vertical diameter HAF ring	*P*=0.947	Horizontal diameter HAF ring	*P*=0.881
Patchy hypoautofluorescence	***P*=0.005**	Peri papillary hypoautofluorescence	***P*=0.039**

Pearson's correlation coefficient for cohorts<30, and Spearman's correlation coefficient for cohorts >30 was performed to evaluate the linear correlation among variables. Bold indicates significant values. BCVA: Best corrected visual acuity, FVD: Foveal vascular density, SCP: Superficial capillary plexus, PFVD: Parafoveal vascular density, FAZ: Foveal avascular zone, OR: Outer retina, IR: Inner retina, EZ: Ellipsoid zone, HAF: Hyperautofluorescence, DCP: Deep capillary plexus , GCC: Ganglion cell complex, CME: central macular edema, CMT: Central macular thickness, MMT: Mean macular thickness

BCVA was significantly correlated with the presence of peri papillary hypoautofluorescence ($P = 0.039$) and patchy hypoautofluorescence ($P = 0.005$).

P1 amplitude in area 1 was greater in patients with normal FAF (1378.5 ± 504.53 mV), and patients with HAF ring had greater P1 amplitude in area 1 (687.96 ± 468 mV) than patients with pattern AF of the fundus (533.33 ± 279 mV). P1 wave amplitude was significantly correlated with the BCVA ($P = 0.004$).

Discussion

In this cross-sectional study, we investigated the macular function, structure, and retinal vessel changes, of patients affected by RP. Overall, we found that RP patients were characterized by alterations of both macular function and structure and that these alterations were associated with retinal vessel changes.

Histopathological studies in RP eyes showed not only photoreceptors and pigment epithelium degeneration but also an important vascular remodeling in both the retina and choroid.[1,2] Since the literature lacks histopathological studies in the early phases of RP, it is still unknown whether vascular changes occur first during the disease, or secondary to the degeneration of pigment epithelium cells and nearby photoreceptors.

In our study, both FVD and PFVD were reduced and the decrease in vascular flow was more pronounced in the parafovea and consistent with the literature.[3] Decreased flow in the SCP and DCP and FAZ enlargement in the latter, are present at an early stage of the disease, thus, vascular alterations may subsequently contribute to the pathophysiology of RP. We believe that the vascular damage in the RP starts at the level of the DCP and then reaches the SCP. Other authors believe that the vascular alterations are concomitant between the DCP and the SCP. Difference in the results can be explained by the different machines used in each study, and different analysis software used (ImageJ in our case). Two theories explain the alteration of both the superficial and deep vascular plexi in RP:

Increased circulating levels of endothelin-1 (ET-1), a potent endogenous vasoconstrictor,[7,8] have been found in patients with RP. Grunwald *et al*.[9] suggested that decreased vascular flow in both plexi happens as a response to decreased metabolic demand of the degenerating photoreceptors and ganglion cells, leading to a reflex capillary vasoconstriction in both plexi mediated by ET-1 as part of a systemic vascular deregulation syndrome.

Makiyama *et al*.[10] demonstrated that the first lesion observed in RP was a decrease in cone density. Despite a good VA and a preserved foveal sensitivity followed by degeneration of bipolar, amacrine, and Muller cells present in the outer plexiform and inner nuclear layers. Later, the flow in the DCP decreases. One way to explain this is that a high metabolic demand resulting for the remodeling and regeneration of the inner nuclear layer may cause a redistribution of blood flow in the DCP located near the inner nuclear layer. Another way to explain this is that reduction of oxygen demand by the photoreceptors may lead to a vascular constriction at the level of the DCP.

The SCP is affected later on during the progression of the disease, Eysteinsson *et al*.[11] suggested that after the death of photoreceptors, oxygen demand of the outer retina decreases significantly and an excessive amount of oxygen reaches the inner retina leading to hyperoxia, a reflex vasoconstriction then occurs at the level of the SCP.[12]

Assuming that vascular changes occur at an early stage of the disease, a reduced flow starting at the level of the DCP and then affecting the SCP may lead to ischemia of the inner retina and to ganglion cell loss. At this stage, loss of photoreceptors in structural OCT may not be obvious, and patients may only have a decreased macular function, undetectable by means of VA measurement and perimetry, the only detectable changes could be identified by means of OCT-A at the microvascular level.

RP is considered as a disease of the photoreceptors and the outer retina; but our study showed that the GCL is also affected, many studies found the same results. Our study states that reduction of superficial and deep flow densities could occur at an early stage of the disease, this would lead to ischemia of the retina and to cell loss both in the outer and inner retina. Thus, preservation of the parafoveal flow in the SCP could be a protective factor of the GCL, and preservation of parafoveal flow in the DCP could be a protective factor of the photoreceptors.

It is important to evaluate, in a longitudinal study, if the relative sparing of retinal capillary plexi could predict a better visual outcome. Furthermore, the cross-sectional nature of this study did not allow us to clarify the cause-and-effect relationship between vascular changes and other structural alterations. Other authors stated that the decreased metabolic demand by the GCC could result in further reduction of blood flow.[3]

In SS-OCT, we found a similar architecture of the macula in all our patients, as described by Hood *et al*.[13] Our study showed that the width of the ELM, still preserved, is always larger than the width of the ellipsoid and that the preservation of the ellipsoid might be correlated with a thicker macula in RP patients. We found that PFVD in the DCP was significantly correlated to the size of the ellipsoid, this is in favor of the hypothesis that alteration in RP begins at the level of the DCP, which affects the outer retina and leads to a narrowing of the ellipsoid. The alteration of the SCP would occur later in the evolution of the disease. The narrowing of the ellipsoid might be an important indicator of disease progression, but its width does not directly reflect VA. To support this hypothesis, we found in our study, patients having a narrow ellipsoid localized only subfoveally but having a good VA.

The hyperreflective FOCI are observed in the retinal layers in various retinal diseases.[14,15] They might reflect local accumulation of microglia in an altered retina, migration of pigment epithelium cells or both. The presence of FOCI may reflect photoreceptor degeneration and subsequent pigment epithelium alteration. Patients with either fragmented or absent ellipsoid have more FOCI than patients with intact ellipsoid, we can state that the presence of FOCI is correlated with an altered ellipsoid.

Several studies[16-19] have shown that the CT is significantly reduced in RP patients. This was not the case in our study where the CT was normal. Choroidal flow density was not investigated. We found a significant correlation between CT and duration of the disease, but not with VA. Hence, the CT could be well correlated to VA, subsequently, in intermediate and advanced stages of the disease, the thinning of the choroid might be correlated with a bad visual function in patients with RP. Sugahara *et al*.[4] showed that the vascular flow in the CC is similar to controls, also, Battaglia Parodi *et al*.[5] found the same results in patients with a RP at an early stage of the disease. Our results are in agreement with the authors who argue that the changes in choroidal vasculature occurs late compared with retinal vascularization, thus a long-term follow-up of these patients is necessary to observe changes in the CT and flow.

It is possible that the VD of the CC does not decrease even if the photoreceptors, pigment epithelium, and the retinal vessels are damaged. This may reflect that the primary lesion in RP occurs in the retinal vascular network, photoreceptors, pigment epithelium but not the choroid. The difference noted could be secondary to the different OCT-A machines used or the differences in the methods of analysis (AngioVue Software, ImageJ software) or to different disease stages and the genetic characteristics of the studied groups. In short, it is possible that, with the progression of RP, gradual alteration of the RPE occurs in the more advanced stages, which improves the penetrance of OCT and OCT-A, thus, the CC appears more clear, whereas in reality flow is decreased.[18]

We found significant correlations between the size of the vertical diameter of the HAF ring and amplitude of P1 in areas 3, 4, and 5. This result was also found in the literature.[20] This shows that the macular function in the area surrounded by the HAF ring is still preserved. The macular function is preserved inside the ring, reduced inside the thickness of the HAF ring and absent outside the latter.

Thus, when the ring is still far from the center of the macula, OCT-A would provide valuable information about the structural damage to the macula. It would be interesting to study the non-functional retina outside the HAF ring by mean of OCT-A, and to evaluate the vascular plexi to know if this retina could be saved when new therapeutic modalities are available.

A major limitation of our study is that the patients had poor genetic characterization. The RP is a heterogeneous disease and every genetic mutation may be responsible for a variety of pathological phenotypes, including specific vascular alterations. This study being transversal, the progression of the RP has not been examined. To measure flow, OCT-A relies on change between two consecutive b-Scans, the machine detects flow only if the difference between the two is superior to a minimum threshold. We could not determine if retinal vessels have totally disappeared, or have just thinned to a level, in which flow is not detectable anymore. Motion blur can affect the quality of images captured by OCT-A and negatively influences the interpretation of vascular densities.

In conclusion, our study showed that vascular changes occur at early stages of the disease and are well correlated to structural

and functional alterations in RP. Since OCT-A is capable of detecting such vascular alterations; it could play a role in staging, prognosis, and progression surveillance of the disease. A protective vascular therapy of the retinal vessels would prevent visual loss in patients with RP.

Financial support and sponsorship

This work was supported by the Tunisian Ministry of Public Health and the Ministry of Higher Education and Scientific Research (LR14SP01).

The author(s) received no financial support for the research, authorship, and/or publication of this article.

Conflicts of interest

There are no conflicts of interest.

References

1. Oishi A, Otani A, Sasahara M, Kurimoto M, Nakamura H, Kojima H, *et al*. Retinal nerve fiber layer thickness in patients with retinitis pigmentosa. Eye (Lond) 2009;23:561-6.
2. Marc RE, Jones BW, Watt CB, Strettoi E. Neural remodeling in retinal degeneration. Prog Retin Eye Res 2003;22:607-55.
3. Toto L, Borrelli E, Mastropasqua R, Senatore A, Di Antonio L, Di Nicola M, *et al*. Macular features in retinitis pigmentosa: Correlations among ganglion cell complex thickness, capillary density, and macular function. Invest Ophthalmol Vis Sci 2016;57:6360-6.
4. Sugahara M, Miyata M, Ishihara K, Gotoh N, Morooka S, Ogino K, *et al*. Optical Coherence tomography angiography to estimate retinal blood flow in eyes with retinitis pigmentosa. Sci Rep 2017;7:46396.
5. Battaglia Parodi M, Cicinelli MV, Rabiolo A, Pierro L, Gagliardi M, Bolognesi G, *et al*. Vessel density analysis in patients with retinitis pigmentosa by means of optical coherence tomography angiography. Br J Ophthalmol 2017;101:428-32.
6. Murakami T, Akimoto M, Ooto S, Suzuki T, Ikeda H, Kawagoe N, *et al*. Association between abnormal autofluorescence and photoreceptor disorganization in retinitis pigmentosa. Am J Ophthalmol 2008;145:687-94.
7. Masaki T, Kimura S, Yanagisawa M, Goto K. Molecular and cellular mechanism of endothelin regulation. Implications for vascular function. Circulation 1991;84:1457-68.
8. Sorrentino FS, Bonifazzi C, Perri P. The Role of the Endothelin System in the Vascular Dysregulation Involved in Retinitis Pigmentosa. J Ophthalmol 2015;2015:405234.
9. Grunwald JE, Maguire AM, Dupont J. Retinal hemodynamics in retinitis pigmentosa. Am J Ophthalmol 1996;122:502-8.
10. Makiyama Y, Ooto S, Hangai M, Takayama K, Uji A, Oishi A, *et al*. Macular cone abnormalities in retinitis pigmentosa with preserved central vision using adaptive optics scanning laser ophthalmoscopy. PLoS One 2013;8:e79447.
11. Eysteinsson T, Hardarson SH, Bragason D, Stefánsson E. Retinal vessel oxygen saturation and vessel diameter in retinitis pigmentosa. Acta Ophthalmol 2014;92:449-53.
12. Padnick-Silver L, Kang Derwent JJ, Giuliano E, Narfström K, Linsenmeier RA. Retinal oxygenation and oxygen metabolism in Abyssinian cats with a hereditary retinal degeneration. Invest Ophthalmol Vis Sci 2006;47:3683-9.
13. Hood DC, Lazow MA, Locke KG, Greenstein VC, Birch DG. The transition zone between healthy and diseased retina in patients with retinitis pigmentosa. Invest Ophthalmol Vis Sci 2011;52:101-8.
14. Nagasaka Y, Ito Y, Ueno S, Terasaki H. Number of hyperreflective foci in the outer retina correlates with inflammation and photoreceptor degeneration in retinitis pigmentosa. Ophthalmol Retina 2018;2:726-34.
15. Kuroda M, Hirami Y, Hata M, Mandai M, Takahashi M, Kurimoto Y. Intraretinal hyperreflective foci on spectral-domain optical coherence tomographic images of patients with retinitis pigmentosa. Clin Ophthalmol 2014;8:435-40.
16. Dhoot DS, Huo S, Yuan A, Xu D, Srivistava S, Ehlers JP, *et al*. Evaluation of choroidal thickness in retinitis pigmentosa using enhanced depth imaging optical coherence tomography. Br J Ophthalmol 2013;97:66-9.
17. Ayton LN, Guymer RH, Luu CD. Choroidal thickness profiles in retinitis pigmentosa. Clin Exp Ophthalmol 2013;41:396-403.
18. Falsini B, Anselmi GM, Marangoni D, D'Esposito F, Fadda A, Di Renzo A, *et al*. Subfoveal choroidal blood flow and central retinal function in retinitis pigmentosa. Invest Ophthalmol Vis Sci 2011;52:1064-9.
19. Sodi A, Lenzetti C, Murro V, Caporossi O, Mucciolo DP, Bacherini D, *et al*. EDI-OCT evaluation of choroidal thickness in retinitis pigmentosa. Eur J Ophthalmol 2018;28:52-7.
20. Robson AG, Tufail A, Fitzke F, Bird AC, Moore AT, Holder GE, *et al*. Serial imaging and structure-function correlates of high-density rings of fundus autofluorescence in retinitis pigmentosa. Retina 2011;31:1670-9.